Transactions on Computer Science and Intelligent Systems Research
ISSN: 2960-1800, eISSN: 2960-2238 | Volume 1
AIEA 2023

Optimal Design of Asynchronous Motor based on Finite Element Simulation

Yongkang Cao

Department of Electrical Engineering, North China Electric Power University, Baoding, China

2587814945@qq.com

Abstract. Aiming at motors' deficiencies such as short life, low efficiency, and high cost in China, this paper optimizes the design of asynchronous motors, so as to improve its performance and efficiency, prolong its life, and reduce its cost. Simulating an asynchronous motor by Maxwell, a finite element simulation software, this paper analyzes the distribution diagrams of waveform and magnetic field including its voltage, current, torque, and back electromotive force to verify the design reliability. Moreover, the parametric simulation of the motor is implemented through the function of Maxwell parameter solver, and the electromagnetic performance under different initial design parameters is simulated. Then, a sensitivity analysis algorithm is adopted to analyze the sensitivity of the motors' initial design parameters. Meanwhile, this paper establishes the platform of motor optimization design, through which the optimization design of motors with different specifications can be fulfilled.

Keywords: Finite Element Simulation; Optimal Design; Motor Optimization; Maxwell; Sensitivity Analysis.

1. Introduction

For a long time, the average life of the motor and the operating system efficiency in China have been 3% ~ 5% and 10% ~ 20% lower than that in foreign countries respectively. Optimizing the motor design will improve its performance and efficiency, prolong its life, and reduce its cost. In this paper, an asynchronous motor is optimized based on finite element simulation.

Scholars at home and abroad have made extensive research on the optimal design of the motor. Targeting the leakage flux paths in the high-speed permanent magnet synchronous motor, the finite element simulation is used in combination with the parametric scanning method to optimize the design of the flux barrier design and the thickness of permanent magnets, which promotes the electrical performance and raises the no-load back electromotive force [1]. An orthogonal test combined with finite element analysis is proposed to solve the problem that the single factor analysis of the three-phase winding inductance of fractional slot permanent magnet motor is not comprehensive with huge differences [2]. Besides, the main influencing factors of three-phase inductance of fractional slot permanent magnet motor are studied, with its difference optimized to meet the engineering design requirements. Aiming at the stress and strain of a high-power motor rotor, the finite element simulation method is used to simulate the stress parameters of the rotor, and the mechanical strength and stiffness of the motor rotor structure are checked simultaneously to analyze the main failure modes of the rotor [3]. Based on the complex and expensive bearingless segment slice motor system, the structure and size of stator elements of the motor are simulated and optimized by finite element simulation. Finally, the optimized rotor position control system of a bearingless slice motor with five stator elements has a fast response speed [4]. Targeting the uneven load distribution of multiple screws in the press-fitting process of the motor core, the finite element method is used to establish a simulation model, study the distribution law of screw load under different loading forces, and optimize the scheme that can obtain uniform screw load [5]. Finite element simulation is adopted with transient magnetic field analysis to calculate the main working indexes such as the electromagnetic torque of the motor. Meanwhile, the influence of the axial length of the stator and rotor on the motor efficiency is investigated to verify the variation law of mechanical

characteristics of the motor [6]. The steady-state characteristics such as the magnetic field distribution of the motor are analyzed by establishing a finite element simulation model. After studying the relationship between the steady-state characteristics and the structural parameters of the motor, the rotor pole and stator pole are widened to optimize the motor and obviously increase its output power [7].Given that the refrigerator will release heat when working, which will raise the temperature and affect the performance of the refrigerator and infrared system, the temperature distribution of each part of the refrigerator is obtained by analyzing the transient thermal simulation of finite elements, thus effectively suppressing the temperature rise of the refrigerator by optimizing its heat dissipation simulation [8]. Based on the difficulty in the design and manufacture of airborne brushless DC motor, the magnetic circuit method is used with finite element simulation to optimize the pole arc coefficient and the number of conductors per slot of the motor. After optimization, the designed motor meets the size, speed, and current requirements of airborne equipment, and the measured back electromotive force is consistent with the simulation results [9]. Given the large torque ripple caused by cogging torque and reluctance torque in built-in permanent magnet synchronous motor, the Taguchi algorithm, genetic algorithm, and finite element analysis are used to realize the multi-objective optimization of rotor structure parameters and parameters with great influence on torque performance [10]. Based on the complex process structure and expensive cost of traditional linear motors, a three-dimensional finite element model of the motor is established by using the direct search algorithm with finite element simulation to obtain the working points of permanent magnets. In addition, the air gap magnetic field characteristics meet the requirements of magnetic circuit design, which verifies the effectiveness of the motor structure [11]. The static and electromagnetic transient simulation models based on finite element analysis are established for the generation mode of the switched reluctance of a double-protrusion electromagnetic generator. The results verify the calculation method of box change parameters, which proves that the commutation parameters are affected by generator speed, load, and excitation current [12]. This paper first implements the finite element simulation to an asynchronous motor through Maxwell, the finite element simulation software. By analyzing the distribution diagrams of waveform and magnetic field including its voltage, current, torque, and back electromotive force to verify its initial design reliability. Secondly, the parametric simulation of the motor is carried out through the function of Maxwell parameter solver, and the electromagnetic performance under different initial design parameters is simulated. Then, a sensitivity analysis algorithm is adopted to analyze the sensitivity of the motors' initial design parameters. Finally, the motor is modeled and optimized by the machine learning algorithm.

2. Initial Design Parameters of the Motor

Table 1. Motor Design Parameters

Motor design parameters	Values and units
Outside diameter of motor stator core	210mm
Inside diameter of motor stator core	136mm
Actual axial length of stator core	145mm
Number of stator slots of motor	35
Outside diameter of motor rotor	135.2mm
Inside diameter of motor rotor	48mm
Number of motor rotor slots	28
Axial length of motor rotor	145mm

In this paper, an asynchronous motor with 7.5 kW as a power and 42.4 N·m as a torque is designed. Motor parameters are shown in Table 1.

Based on the above design parameters, the punching diagram can be seen as follows:

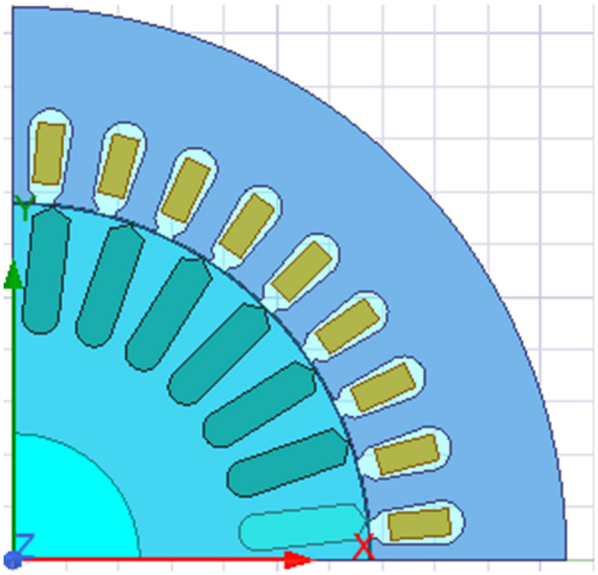

Figure 1. Motor Punching Diagram

3. Finite Element Analysis and Calculation of Motor

To verify the rationality of the electromagnetic parameters of the motor's initial design, this paper will analyze the rationality of the initial design of the motor through Maxwell for the existing design parameters.

3.1. Finite Element Method

As a numerical analysis method, the finite element method (FEM) is used to solve mathematical models of various physical problems. By dividing the complex continuum into a series of finite subdomains (called finite elements), and establishing appropriate approximate functions on each subdomain, the original problem is transformed into a discrete algebraic one and then solved numerically.

The basic steps of the finite element method are as follows:

1. Mathematical modelling. According to practical problems, a mathematical model of problems should be established, including defining geometric shapes, boundary conditions, material characteristics, and loading conditions.

2. Mesh modelling. The model is divided into finite elements to form a finite element mesh. According to the characteristics and requirements of the problem, appropriate element types are chosen, such as triangle, quadrilateral, hexahedron, etc.

3. Algebraic equation solving. Numerical methods are used to solve algebraic equations, usually using iterative or direct solutions, such as the Gaussian elimination method and conjugate gradient method.

4. Post-processing. The numerical solution is post-processed, including calculating and analyzing the interested physical quantities, visualizing the results, evaluating the accuracy and precision of the solution, etc.

3.2. Principle of Finite Element Analysis of Motor

Based on the above finite element analysis principle, finite element analysis is implemented for the motor, with specific analysis steps as follows.

1. Establish the geometric model of the motor. In Maxwell, according to the collected geometric information, the geometric model of the motor should be established.

2. Define motor materials. In Maxwell, it is necessary to define appropriate material properties for each part, such as conductivity, permeability, and loss of the wire, insulating material, and core material.

3. Define the boundary conditions of the motor. According to the working and boundary conditions of the motor, appropriate constraints and excitation should be defined, including the power supply conditions, winding current, air gap, and fixed boundary conditions of the motor.

4. Divide the finite element mesh. The geometric model of the motor should be divided into small finite element elements to form the finite element mesh. Maxwell provides a variety of mesh partition options, where the appropriate mesh type and size can be chosen according to your needs.

5. Analyze the electromagnetic field. Maxwell solver is used to solve the electromagnetic field equation on the finite element mesh. The electromagnetic characteristics of the motor, such as magnetic field distribution, induced electromotive force, torque, three-phase current, etc. need considerations in the solution.

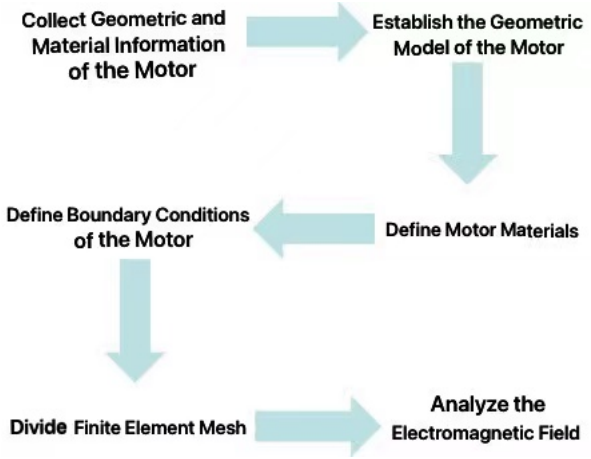

Figure 2. Flow Chart of Finite Element Analysis of Motor

3.3. Finite Element Modeling and Result Analysis of Motor

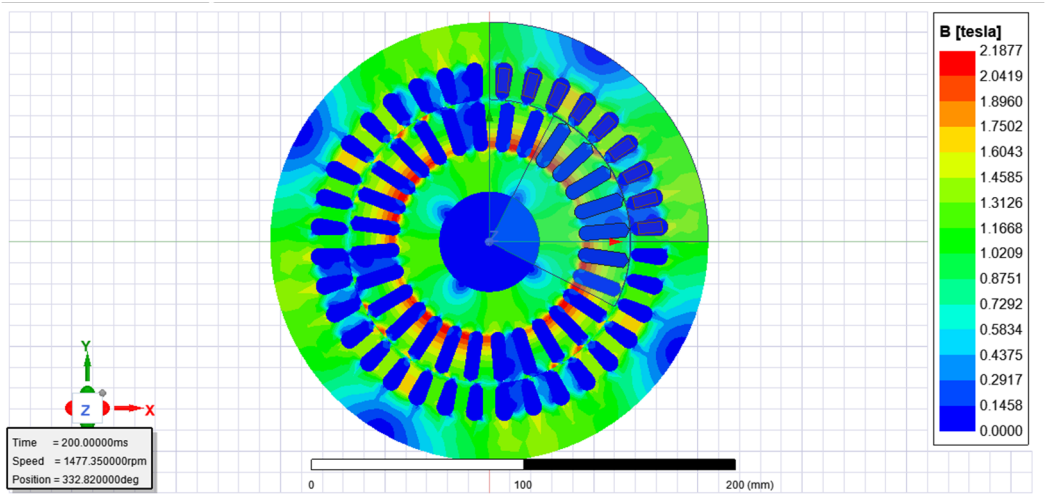

Figure 3. Distribution of Magnetic Flux Density

According to the above figure, the maximum of the rotor is 2.1877 T and is mainly distributed in the yoke of the rotor, while the maximum of the stator is about 1.6043 T and is mainly distributed in the slot of the stator. The initial design of the motor accords with the basic conditions of flux density distribution.

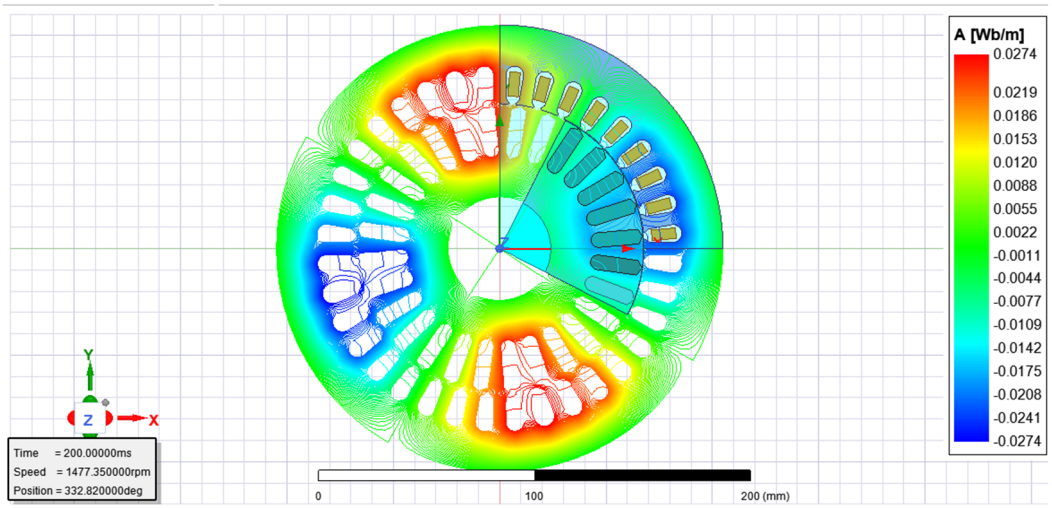

Figure 4. Distribution Diagram of Vector Magnetic Potential

According to the above figure with the maximum of 0.0274 Wb/m and the minimum of -0. 0274 Wb/m, the overall magnetic flux leakage is less, and the distribution of magnetic lines of force is also obvious.

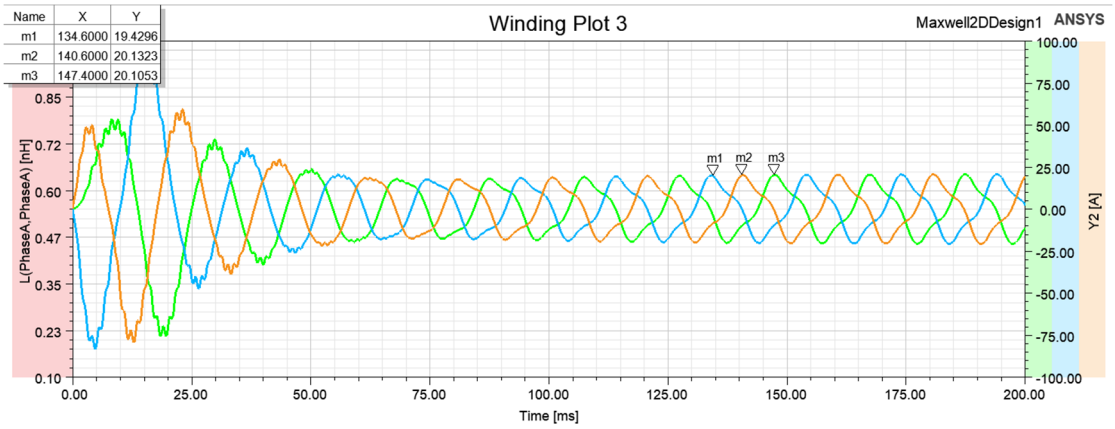

Figure 5. Three-Phase Current Winding Plot

According to the above figure, after 55ms, the waveform tends to be stable and finally presents a sine wave current with approximate three-phase symmetry.

Before stabilization, the waveform will oscillate, which may be due to the electromagnetic oscillation in the starting process. When the asynchronous motor starts, the starting electromagnetic force of the motor rotor may cause the motor oscillation. This is due to the electromagnetic force in the motor on the rotor caused by the oscillation, which will be manifested by the periodic changes in the current.

As can be seen from the figure, after stabilization, the three-phase symmetrical current will appear burr, which may be caused by the characteristics of the motor itself. When the asynchronous motor is running, its characteristics may lead to the current waveform burr. For example, the nonlinear magnetic circuit, saturation phenomenon, capacitance, and inductance of the motor may trigger the distortion of the current waveform.

According to the above figure, the torque tends to be stable after 135ms, which is about 43N·m after stabilization.

Before stabilization, the waveform will oscillate, which may result from the mechanical coupling in the starting process. When the asynchronous motor starts running, a certain mechanical coupling exists between the motor and the load, which will trigger the instability of torque transmission. For example, at startup, there may be inertia differences between the rotor and the load of the motor, which may oscillate the torque waveform.

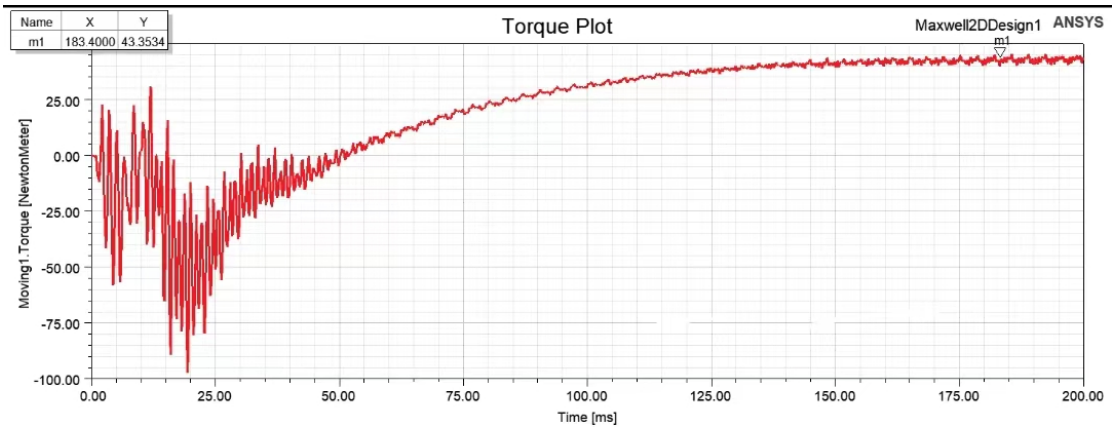

Figure 6. Torque Waveform Distribution Diagram

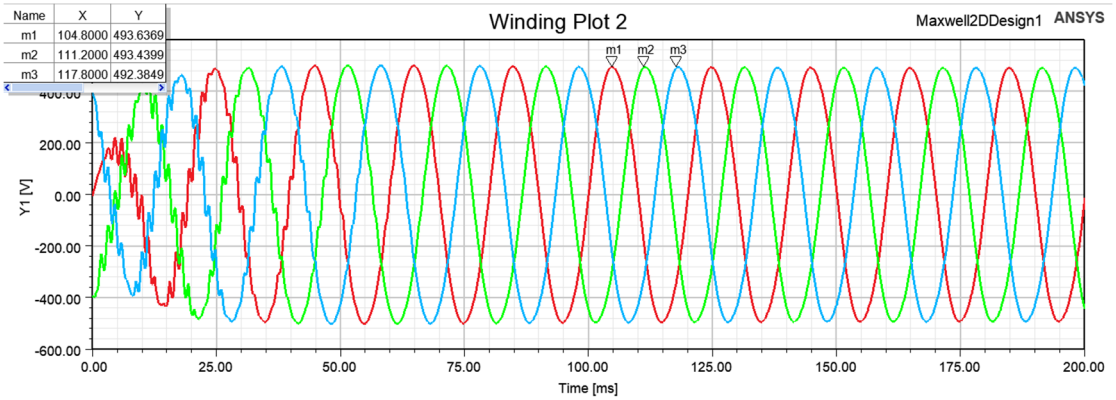

Figure 7. Winding Plot of Three-Phase Back Electromotive Force

According to the above figure, the waveform tends to be stable after 40ms, which finally presents a three-phase symmetrical sine wave current. To sum up, the motor's initial performance meets requirements and the initial design is reasonable.

4. Parametric Simulation of Motor

4.1. Principle of Parametric Simulation of Motor

Parametric simulation of a motor is a method to represent the behavior and performance of a motor by establishing a mathematical model to simulate and analyze the model. In the parametric simulation of the motor, various parameters of the motor such as resistance, inductance, torque, speed, etc. are converted into mathematical variables for simulation and analysis.

Different performance simulations of the motor can be obtained by changing the parameters. This simulation method can evaluate, optimize, and verify the motor in the design and development, which reduces the experimental cost and development cycle, improves the performance and reliability of the motor, and saves resources.

4.2. Principle of Maxwell Finite Element Analysis

The Optimmetrics module of Maxwell can be used to realize simulation under different initial design parameters. The change of a specific parameter causes the change of other parameters on motor performance, forming a series of simulation schemes, from which the relatively better scheme can be selected.

The selection of motor parameters in this paper is shown in the following.

Design Variable	Override	Value	Units
b	☐	3.5	mm
bb	☐	6.2	mm
fractions	☐	4	
h	☐	0.8	mm
hh	☐	1.5	mm
rb	☐	1	mm
rbb	☐	6.9	mm
rh	☐	0.5	mm
rhh	☐	1.7	mm
rr	☐	136	mm

Figure 8. Selection of Parameters

4.3. Parametric Analysis based on Maxwell

4.3.1. Parameterized Variable Selection

The change of stator slot and rotor slot will affect the uniform distribution of air gap and then the flux density distribution, which will affect the electromagnetic performance of the motor. The change in the inside diameter of the stator core will affect the air gap of the motor, thus affecting its electromagnetic performance. Therefore, the corresponding parameters of the stator slot are selected: the corresponding parameter of Hs0 is h, that of Hs1 is hh, that of Bs0 is b, and that of Bs1 is bb. The corresponding parameters of the rotor slot are selected: the corresponding parameter of Hs0 is rh, that of Hs1 is rhh, that of Bs0 is rb, that of Bs1 is rbb, and that of stator core inside diameter DiaGap is rr.

4.3.2. Parametric Analysis Results

This paper mainly studies the motor torque and three-phase current. For example, the torque and three-phase current winding plots for parameter b are shown below.

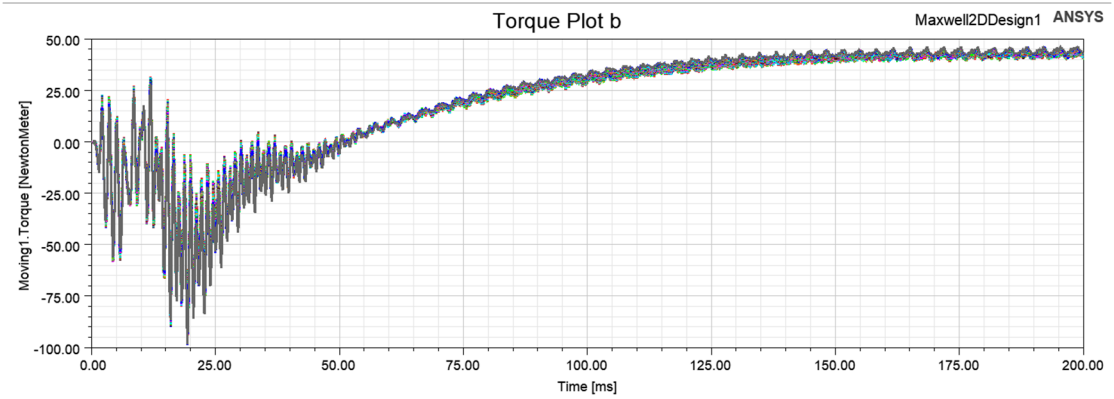

Figure 9. Torque Winding Plot of Parameter b

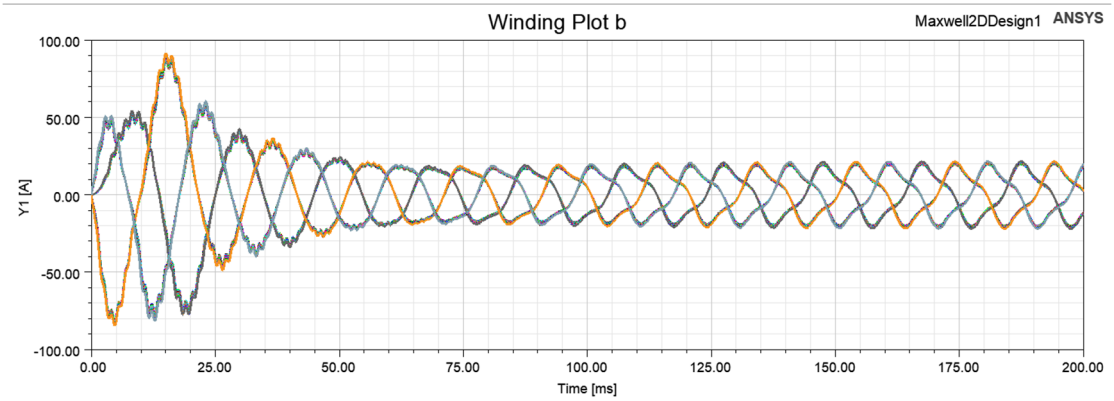

Figure 10. Three-Phase Current Winding Plot of Parameter b

Because of the symmetry of three-phase currents, only one of them is taken for study.

Table 2. Simulation Results of Parameter b and Parameter bb

b(mm)	Current (A)	Torque (N·m)	bb(mm)	Current (A)	Torque (N·m)
2.95	20.0571	19.1200	5.6	20.1253	19.3799
3.05	20.1073	19.1671	5.7	20.1575	19.3777
3.15	20.1569	19.2132	5.8	20.1902	19.3759
3.25	20.2016	19.2531	5.9	20.2238	19.3758
3.35	20.2521	19.3001	6.0	20.2573	19.3759
3.45	20.3037	19.3545	6.1	20.2923	19.3758
3.5	20.3282	19.3769	6.2	20.3282	19.3769
3.55	20.3622	19.4173	6.3	20.3656	19.3802
3.65	20.4185	19.4693	6.4	20.4041	19.3847
3.75	20.4675	19.5080	6.5	20.443	19.3873
3.85	20.5164	19.5456	6.6	20.4841	19.3900

Table 3. Simulation Results of Parameter h and Parameter hh

h(mm)	Current (A)	Torque (N·m)	hh(mm)	Current (A)	Torque (N·m)
0.4	20.5455	19.3670	1.15	20.4367	19.3554
0.5	20.485	19.3659	1.25	20.4036	19.3594
0.6	20.4302	19.3685	1.35	20.3721	19.3690
0.7	20.3796	19.3718	1.45	20.3424	19.3741
0.8	20.3282	19.3769	1.5	20.3282	19.3769
0.9	20.2895	19.3989	1.55	20.3154	19.3806
1.0	20.2462	19.4063	1.65	20.2903	19.3922
1.1	20.199	19.4036	1.75	20.2645	19.3973
1.2	20.1718	19.4323	1.85	20.2367	19.3969

Table 4. Simulation Results of Parameter rb and Parameter rbb

rb(mm)	Current (A)	Torque (N·m)	rbb(mm)	Current (A)	Torque (N·m)
0.6	20.1386	18.8648	4.9	18.3534	18.6328
0.7	20.1877	19.0351	5.4	18.8454	18.8485
0.8	20.2279	19.1770	5.9	19.3382	19.0512
0.9	20.2914	19.2400	6.4	19.8331	19.2218
1.0	20.3282	19.3769	6.9	20.3282	19.3769
1.1	20.3733	19.4520	7.4	20.8488	19.5251
1.2	20.4177	19.4974	7.9	21.3898	19.6439
1.3	20.4615	19.5294	8.4	21.9571	19.7531
1.4	20.5073	19.5422	8.9	22.5838	19.7735

Table 5. Simulation Results of Parameter rh and Parameter rhh

rh(mm)	Current (A)	Torque (N·m)	rhh(mm)	Current (A)	Torque (N·m)
0.3	20.5107	19.5719	1.2	20.4592	19.4479
0.35	20.4666	19.5053	1.3	20.4346	19.4209
0.4	20.4117	19.4610	1.4	20.4052	19.4096
0.45	20.3733	19.4124	1.5	20.3711	19.4038
0.5	20.3282	19.3769	1.6	20.3507	19.3816
0.55	20.2872	19.2828	1.7	20.3282	19.3769
0.6	20.241	19.3055	1.8	20.3087	19.3774
0.65	20.1982	19.2712	1.9	20.2824	19.3830
0.7	20.147	19.2432	2.0	20.2753	19.3747
0.75	20.1119	19.1982	2.1	20.2542	19.3735

Table 6. Simulation Results of Parameter rr

rr(mm)	Current (A)	Torque (N·m)
136	20.3282	19.3769
136.5	21.1408	20.0873
137	21.8986	20.3720
137.5	22.6434	20.4846
138	23.3692	20.4823
138.5	24.0923	20.4348
139	24.8134	20.3527
139.5	25.5366	20.2517
140	26.2654	20.1338

5. Sensitivity Analysis of Motor

5.1. Principle of Sensitivity Analysis

Sensitivity analysis refers to the process of evaluating and analyzing how the change of input variables influences the output results of a model or system. In addition to helping us understand the behavior of the system, it can evaluate the importance of each input variable to the output and provide guidance for system design and optimization. The principle of sensitivity analysis mainly includes the selection of input variables, the change of variable values, the solution of the model, the output analysis, and the sensitivity analysis.

5.2. Sensitivity Analysis Results

According to the sensitivity analysis criteria, formula (1) can be obtained:

$$A = \left| \frac{X_t - X_1}{t-1} \right| \quad (1)$$

The sensitivity of each variable can be calculated by formula (1), in which the value A represents sensitivity, the larger the A, the stronger the sensitivity of the variable. X_t is the last term of the simulation result of a single parameter variable, X_1 is the first term of the simulation result of a single parameter variable, and $t-1$ is the difference between the last term and the change before the first term.

For parameter b: $A_{current}$ = 0.51, A_{torque} = 0.47

For parameter bb: $A_{current}$ = 0.36, A_{torque} = 0.01

For parameter h: $A_{current}$ = 0.47, A_{torque} = 0.08

For parameter hh: $A_{current}$ = 0.29, A_{torque} = 0.06

For parameter rb: $A_{current}$ = 0.46, A_{torque} = 0.85

For parameter rbb: $A_{current}$ = 1.06, A_{torque} = 0.29

For parameter rh: $A_{current}$ = 0.89, A_{torque} = 0.83

For the parameter rhh: $A_{current}$ = 0.23, A_{torque} = 0.08

For parameter rr: $A_{current}$ = 1.48, A_{torque} = 0.19

It can be concluded that the stator diameter has the strongest sensitivity to current, and the rotor slot width has the strongest sensitivity to torque. This research can be optimized in different industrial application scenarios for different requirements.

6. Conclusion

Firstly, this paper simulates the initial design parameters of an asynchronous motor by the finite element method. Through the calculation of voltage, current, torque, back electromotive force, and magnetic field distribution, the maximum flux density of the rotor is 2.1877 T, which is mainly distributed in the yoke of the rotor, while the maximum flux density of the stator is about 1.6043 T, which is mainly distributed in the slot of the stator. After the torque is stabilized, the value is about 43 N·m. Meanwhile, after the current is stabilized, it is about 20A, which meets the design standard. Secondly, the parametric simulation of the motor is implemented through the function of Maxwell parameter solver, and the electromagnetic performance under different initial design parameters is simulated. Finally, the sensitivity analysis of the initial design parameters of the motor is carried out through the sensitivity analysis algorithm. It is concluded that the stator inside diameter has the strongest sensitivity to the current, and the rotor slot width has the strongest sensitivity to the torque. This design scheme can optimize the design for different motors and improve the utilization efficiency of motors in different application scenarios.

References

[1] Zhang, D., Xie, Q. Q., Xu, H. F. et al. (2022). Optimal design of electric performance of high-speed PMSM. Explosion-Proof Electric Machine, (002): 057.

[2] Zhang, C., Zhang, M., Guo, J. X. et al. (2018). The fractional slot permanent magnet motor's inductance optimization based on orthogonal experiment. Journal of Detection & Control, 40(04), DOI:CNKI:SUN:XDYX.0.2018-04-016.

[3] Fu, C. M., Mao, W. G. & Xiao, X. Z. (2009). Finite element simulation and the structure optimization of the rotor of YKSL2150 electrical machine. Journal of Hunan University of Science and Technology (Natural Science Edition), 24(3), 5. DOI:10.3969/j.issn.1672-910 2.2009.03.007.

[4] Zhao, J. Y., Zhao, X. H. & Wang, X. L. (2015). Design and optimization of bearingless segment slice motor with five stator elements. Micromotors, 48(7), 5. DOI:10.3969/j.issn.1001-68 48.2015.07.007.

[5] Li, H. D., Xi, J. T. & Guo, Y. B. (2014). Simulation and optimization for the press-fit process of large motors cores. Machinery Design & Manufacture, (1), 4. DOI:10.3969/j.issn.1001-399 7.2014.01.059.

[6] Cheng, T., He, Y., Chen, X. A. et al. (2013). Electromagnetic field analysis and parameter optimization for an asynchronous motorized spindle motor with finite element method. Machinery, 40(2), 6. DOI: CNKI: SUN: MECH. 0. 2013-02-004.

[7] Hang, J. Y., Chen, Z. H., Zou, X. Y. et al. (2013). Simulation and optimization of four-phase wound field doubly salient generator. Mircromotors, 46(8), 5. DOI:10.3969/j.issn.1001-6848. 2013.08.005.

[8] Xin, G. L., Chi, G. C., Rao, Q. C. et al. (2020). Thermal simulation and heat dissipation optimization of rotary stirling cryocoolers. Cryogenics & Superconductivity, (2): 5. DOI:CNKI: SUN:DWYC.0.2020-02-003.

[9] Cao, K., Wan, Y. H. & Wang, J. F. (2013). Simulation and optimization on the design of an airborne brushless DC motor. Electrical Machinery Technology, (5), 5. DOI:10.3969/j.issn 1006-2807.2013.05.005.

[10] Hu, K., Wei, M., Zhuang, H. J. et al. (2020). Optimization design of interior permanent magnet synchronous motor based on compound algorithm. Mircromotors, 53(11), 6.

[11] Liu, J. L. (2012). Optimal design and simulation of low-speed permanent magnet linear motor. Zhengzhou: Master's Dissertation of Zhengzhou University.

[12] Dai, W., Han, G., Wang, H. et al. (2010). Commutation analysis of doubly salient electro-magnetic generator in SRG mode with finite element computer simulation. International Conference on Computer Application & System Modeling. IEEE. DOI:10.1109/ICCASM. 2010.5619059.